Preventive effects of *Dendrobium* hybrid extract on free radical activity and melanoma cell proliferation by inducing apoptotic gene expression

RUNGPAILIN KHONSAP[1], PILAIRATH MEKSANGSEE[1], PICHAMON KIATWUTHINON[1], NATTANAN PANJAWORAYAN T-THIENPRASERT[1], NAPACHANOK MONGKOLDHUMRONGKUL SWAINSON[1], WANNARAT PHONPHOEM[1], PAKORN WATTANA-AMORN[2,3] and ATTAWAN ARAMRAK[1]

[1]Department of Biochemistry, Faculty of Science, Kasetsart University, Bangkok 10900, Thailand; [2]Department of Chemistry, Faculty of Science, Kasetsart University, Bangkok 10900, Thailand; [3]Special Research Unit for Advanced Magnetic Resonance and Center of Excellence for Innovation in Chemistry, Faculty of Science, Kasetsart University, Bangkok 10900, Thailand

Received July 2, 2025; Accepted October 13, 2025

DOI: 10.3892/br.2025.2094

Abstract. *Dendrobium* species are used in folk medicines due to their medicinal properties by acting as antioxidants and anticancer agents. Derived from parent plants used in dermatological treatments and cosmetics, *Dendrobium* Pearl Vera hybrid (DH) was extracted and investigated for its inhibitory effects on free radicals and skin cancer cell proliferation. Based on colorimetric spectrophotometry, the propanolic extract (DH-P) from the whole plant contained flavonoids, phenolics and alkaloids at 80.11±0.69, 50.51±0.44 and 38.75±1.77 μg/g fresh weight, respectively. Using high-resolution mass spectrometry, eight compounds involved in skin protection were annotated: Fuanosine, L-glutamine, threonic acid, quercetagetin, shikimic acid, mannose, *p*-coumaric acid and L-malic acid. DH-P scavenged free radicals in a concentration-dependent manner and inhibited the activity of collagenase and hyaluronidase, but not in a concentration-dependent manner. Treatment using DH-P for 96 h significantly decreased the proliferation of SK-MEL-28 melanoma cells in a dose-dependent manner, with a half-maximal inhibitory concentration of 20.23±1.04 μg/ml. Thus, DH-P at 20 μg/ml was used in further studies. Cell migration was not inhibited by DH-P. However, DH-P may induce SK-MEL-28 cell death through apoptosis, as nuclear condensation and fragmentation was observed after 48 h DH-P treatment. Gene expression analysis was performed to evaluate key signaling molecules involved in cell apoptosis, such as *bax*, *bcl-2*, *cytochrome c*, caspases (*cas)-3* and *-9* and *p53*. The expression levels of *cas-3* and *cas-9*, executors in the apoptosis pathway, were significantly upregulated in the SK-MEL-28 cells treated with DH-P for 48 h, further confirming that cell death may occur through an apoptosis mechanism.

Correspondence to: Professor Attawan Aramrak, Department of Biochemistry, Faculty of Science, Kasetsart University, 50 Ngamwongwan Road, Lat Yao, Chatuchak, Bangkok 10900, Thailand
E-mail: fsciawa@ku.ac.th

Key words: anti-cancer, anti-oxidant, apoptosis, natural product, orchid, phytochemical, skin cancer

Introduction

Orchids belong to the family Orchidaceae, one of largest families of flowering plant and the most diverse family with >25,000 species in ~880 genera (1). Several orchids have been used for a variety of purposes, including ornamental plants, sources of natural antioxidants and bioactive compounds and for cosmeceutical use (2). *Dendrobium* spp. is a large genus with >1,000 species that can grow in a variety of environments and as epiphytes in tropical and subtropical Asia and eastern Australia (3). Several *Dendrobium* species have been used in traditional medicine due to the high number of bioactive compounds, such as polyphenols, flavonoids, alkaloids and polysaccharides (3,4). These compounds have key biological activities. For example, phenolics and flavonoids exhibit antioxidant capacity, which could promote human health and prevent chronic and degenerative diseases, including cancer, caused by free radicals (5). *D. crepidatum* contains bibenzyl derivatives, polyphenols and flavonoids that have antioxidant and cytotoxic effects on cancer cells (6). *D. denneanum* and *D. nobile* contain bioactive polysaccharides and exhibit antioxidant properties (7,8).

Skin cancer is one of the most frequent malignancies worldwide and can be classified into melanoma skin cancer (MSC) and non-MSC (9). According to global data from 2000 to 2024, MSC ranks 17th in prevalence and 23rd as a leading cause of cancer-related death, with the highest incidence and mortality rate reported in Europe. While Asia has the lowest incidence rate of MSC, it records the second-highest mortality rate (9). In humans, malignant melanoma cells consist of activating mutations of B-RAF oncogene, resulting in abnormal cell proliferation (10). The SK-MEL-28 cell line is a type of human malignant melanoma cell and the most aggressive form of skin

cancer. The migration and invasion of melanoma cells are involved with proteolytic enzymes such as serine and cysteine proteases and matrix metalloproteases (MMPs) in remodeling dermal extracellular matrix (ECM) (11). The ECM comprises a large variety of macromolecules, including fibrous-forming proteins (collagen and elastin) and carbohydrate strings (proteoglycans, glycosaminoglycans and glycoproteins), and enzymes (proteinases and MMPs). Collagens are predominant and the main targets for MMPs, especially collagenases, in ECM remodeling (11,12). Also, the accumulation of hyaluronan (HA), a polysaccharide subfamily of glycosaminoglycans, is attributed to the progression and metastasis of cancer cells (13). *D. draconis*, *D. falconeri*, *D. findlayanum* and *D. loddigesii* have been reported for their ability to inhibit the proliferation of numerous types of cancer cell (14), including colon cancer (15) and leukemia (16). Most cancer cells are inhibited by many pathways, including autophagy and apoptosis (both intrinsic and extrinsic). Secondary metabolites, such as bibenzyl compounds from *D. loddigesii*, induce apoptosis in melanoma cells (17). In addition, the crude extract and certain compounds isolated from *Dendrobium* have been found to regulate the changes of expression of genes and proteins involved in apoptosis, especially in the intrinsic pathway (18-23). The *bcl-2* gene family is a key factor in the regulation of cell apoptosis, including anti-apoptotic genes (*bcl-2* and *bcl-XL*) and pro-apoptotic genes (*bax* and *bid*) (18). Some traditional Chinese medicine anticancer drugs have been found to induce cell apoptosis through targeting the proteins of the bcl-2 family and increasing the ratio of *bax* to *bcl-2* (19). *D. officinale* extracts increase the protein levels of Bax and caspase-3 and decreased Bcl-2 in extract-fed rats with gastric cancer (20). *D. officinale* extract primarily contains polysaccharides, including mannose, which exhibit anti-tumor activity and induce apoptosis in osteosarcoma cells via caspase upregulation (21). Moreover, Nudol, a phenanthrene derivative from *D. nobile*, notably enhances the mRNA expression levels of *cytc* and *caspases* in osteosarcoma cells (22). Quercetin, a flavonoid compound commonly found in plant extracts, exerts anti-cancer activity by inducing nuclear fragmentation and intrinsic apoptosis via an increase in *p53* expression (23).

Our previous study investigated orchid hybrids that were primarily created for horticultural purposes and found that the propanolic extract from *Dendrobium* Pearl Vera [a *Dendrobium* hybrid; DH-P] exhibited antioxidant activity and could reduce melanin production and viability of melanoma SK-MEL-28 cells treated with phenolic contents at 15 μg/ml (24). To the best of our knowledge, however, there are no published reports on the bioactive compounds in such *Dendrobium* hybrids. Swainson *et al* (24) identified certain annotated bioactive compounds using high-resolution mass spectrometry (HR-MS) coupled with the Orbitrap (ion trap-based mass analyzer) using an untargeted approach. Quadrupole time-of-flight (QTOF) is one of the most popular mass analyzers used in analytical screening of targeted and non-targeted substances due to its robustness, high sensitivity and specificity. The present study aimed to identify other bioactive compounds in the DH plant using QTOF and determine the effects of DH-P on free radicals, enzyme activity involved in ECM, cell migration and the mechanism of SK-MEL-28 cell death at the gene level.

Materials and methods

Chemicals and reagents. The standards used for the HR-MS experiment were quercetin (Sigma-Aldrich; Merck KGaA; cat. no. Q4951), dendrobine (Chengdu Biopurify Phytochemicals, Ltd.; cat. no. BP0479) and gigantol (Sigma-Aldrich; Merck KGaA; cat. no. Sml2036). The human melanoma cell line was SK-MEL-28 (American Type Culture Collection; cat. no. HTB-72). Other chemicals, reagents and media used were HPLC, analytical or molecular biology grade, as appropriate.

Preparation of DH-P. DH plants (a hybrid between *Dendrobium* Topaz Dream and *D. bigibbum*; CordyBiotech Co., Ltd.) were cultured *in vitro* for 3-4 months in Murashige and Skoog medium (PhytoTech Labs; cat. no. M524) containing 6.8 g/l agar and 17 g/l sucrose, at 25±2˚C under 300 lux light for 16 h/day. Whole plants of DH were harvested and ground using liquid nitrogen. The ground sample was extracted using 2-propanol with a ratio of 1:5 (w/v). Samples were macerated at room temperature for 24 h. The filtrate was collected through filter papers (Whatman plc; Cytiva; cat. no. 1001-090) and samples from three extractions were pooled. The filtrate was concentrated using a rotary evaporator and lyophilized. The extraction was performed twice independently. DH-P was redissolved in 95% ethanol for further use.

Screening of secondary metabolites using thin-layer chromatography (TLC). DH-P was prepared to a final concentration of 10 mg/ml in 95% ethanol. Then, extract samples were subjected to TLC analysis for the presence of phenolics and flavonoids as previously described (25). Quercetin was used as a reference for detection. A total of ~5 drops/sample were applied on a 10x5 cm silica gel plate (Merck KGaA) and separated in a mobile phase consisting of a ratio of ethyl acetate-to-acetic acid-to-water of 8:1:1 (v/v/v). The gel plate was sprayed with 0.1% 2-aminoethyl diphenylborinate solution to visualize phenolics and flavonoids using ultraviolet viewing cabinets (Spectronics Corporation) at 366 nm.

Measurement of total phenolic content. The total phenolic content in DH-P was determined in a microwell plate as previously described with modification (26). In total, 20 μl standard or DH-P were added, followed by 100 μl 10% v/v Folin-Ciocalteu solution in 96-well plates at room temperature for 3 min; then, 80 μl 1 M sodium carbonate was added at room temperature for 20 min. The absorbance was measured at 765 nm using a microplate reader (Tecan Group, Ltd.; cat. no. M200). Gallic acid (GA) was used as a standard. Each sample was performed in triplicate. The total phenolic content was reported as μg GA equivalent (E)/g tissue.

Measurement of total flavonoid content. Total flavonoid content in DH-P was determined in a microwell plate as previously described with a slight modification (27). Distilled water (104 μl) was mixed with 60 μl methanol in each well. Then, 20 μl standard or DH-P and 8 μl 0.5 M potassium acetate solution were added, followed by 8 μl 5% (w/v) aluminum chloride solution. The mixture was shaken in an orbital shaker (Edmund Bühler GmbH) for 5 min and incubated in the dark at room temperature for 30 min. The absorbance was measured

at 415 nm. Quercetin was used as a standard. Each sample was performed in triplicate. The total flavonoid content was reported as μg quercetin equivalent (QE)/g tissue.

Measurement of total alkaloid content. The total alkaloid content in DH-P was determined as previously reported (28). A sample (1 ml) of standard or DH-P was transferred to a separating funnel and mixed with 5 ml each bromocresol green solution and phosphate buffer (pH 4.7). The complex was extracted with 10 ml chloroform using sequential addition of 1, 2, 3 and 4 ml. The extracted complex was collected from each addition, pooled and measured for absorbance at 470 nm. Atropine was used as a standard. Each sample was performed in triplicate. The total alkaloid content was reported as μg atropine equivalent (AE)/g tissue.

Identification of compounds using ultra-high-performance liquid chromatography (UHPLC)-electrospray ionization-QTOF-tandem mass spectrometry (ESI-QTOF-MS/MS). DH-P at a concentration of 1 mg/ml in 95% ethanol was filtered through a 0.2 μm nylon filter. The composition was separated using UHPLC-ESI-QTOF-MS. A pure compound (dendrobine, gigantol and quercetin) was used as a reference. These compounds have been reported to accumulate in *Dendrobium* species and exhibit antioxidant and anticancer properties (4,23). The standard was prepared at a final concentration of 20 μg/ml in methanol. All samples were analyzed by the Scientific Equipment Center (Kasetsart University, Thailand). The chromatographic separation and parameters were set up for the detection of dendrobine, gigantol and quercetin as previously described (29-31). An ExionLC™ AD system (AB Sciex LLC) equipped with a C18 column (100.0x4.6 mm; internal diameter, 2.6 μm; Phenomenex, Inc.) was used for separation. Metabolite analysis of the matrix was performed on a SCIEX X500R QTOF system with Turbo V™ source (AB Sciex LLC) using the ESI probe operated in either positive or negative ion mode. Information-dependent acquisition was also performed on the X500R QTOF system. The TOF MS (scan range, 100-500 Da) parameters were as follows: declustering potential (DP), 50 V; collision energy (CE), 10 V and accumulation time, 0.25 sec for positive mode and DP, -60 V; CE, -10 V and accumulation time, 0.25 sec for negative mode. The TOF MS/MS (scan range 50-500 Da) parameters were DP, 50 V; CE, 35 V; CE spread (CES), 0 V and accumulation time, 0.1 sec for the positive mode, but DP, -60 V; CE, -35 V; CES, 0 V; accumulation time, 0.1 sec for the negative mode. MS/MS fragmentation patterns of compounds detected in the crude extract were compared with those in the National Institute of Standards and Technology research library (version 2017; https://chemdata.nist.gov/). Compounds with a mass error within ±5 ppm were selected as putative metabolites present in DH-P.

2,2-Diphenyl-1-picrylhydrazyl (DPPH) radical scavenging capacity. DPPH assay was performed in a microplate as previously described, with minor modification (32). A sample (25 μl) of the control or DH-P was added in each well with 160 μl 150 μM DPPH radical solution (Sigma Aldrich; cat. no. D9132). The mixture was incubated in the dark at room temperature for 30 min. The scavenging activity of the samples against DPPH radicals was detected at 517 nm. Each sample was run in triplicate. Ethanol was used as a background control. Ascorbic acid was used as a positive control and standard. Scavenging activity was calculated based on the absorbance (A) as follows: % Radical scavenging=(1-A_{sample}/$A_{control}$) x100. Antioxidant activity was expressed as vitamin C equivalent antioxidant capacity (VCEAC) in μg/ml.

2,2'-Azino-bis(3-ethylbenzothiazoline-6-sulfonic acid) (ABTS) radical scavenging capacity. ABTS assay was performed in a microplate as previously described, with minor modification (33). The working solution was prepared by mixing 0.5 ml $ABTS^+$ (Applichem; cat. no. A1088) with 30 ml methanol at a ratio of 1:60 v/v. The absorbance at 734 nm was determined to be 1.1±0.02 AU before use in the experiment. The reaction was performed by mixing 10 μl control or DH-P with 190 μl $ABTS^+$ working solution at room temperature for 2 h. The scavenging activity was detected at 734 nm. Each sample was run in triplicate. Ethanol was used as a background control. Ascorbic acid was used as a positive control and standard. ABTS scavenging activity was calculated as for DPPH.

Ferric reducing antioxidant power (FRAP). FRAP assay was performed in a microplate as previously described with a minor modification (34). A total of 10 μl control or DH-P was added with 140 μl FRAP solution in the dark at 37˚C for 30 min. The absorbance of the mixture was read at 593 nm. Each sample was run in triplicate. Ethanol was used as a background control. A standard curve was generated using ascorbic acid (0-1,000 μM) and used for calculation of the antioxidant activity. Reducing power was reported as the FRAP value/mg extract.

Inhibition of collagenase activity. Collagenase inhibition assay was performed using Collagenase Activity Colorimetric Assay kit (Sigma-Aldrich; Merck KGaA; cat. no. MAK293) according to the manufacturer's instructions. The mixture was prepared by adding collagenase assay buffer and DH-P sample or inhibitor control (1 M 1,10-phenanthroline). Ethanol was used as a background control. The mixture was added with 5 μl 0.35 U/ml collagenase enzyme at room temperature for 10 min. A total of 20 μl 1 mM N-[3-(2-furyl)acryloyl]-L-leucyl-glycyl-L-prolyl-L-alanine substrate and 30 μl collagenase buffer were added. The reaction was immediately measured in the kinetic mode at absorbance of 345 nm and 37˚C for 5-15 min. Each sample was performed in triplicate. Collagenase inhibition was calculated according to the manufacturer's instructions.

Inhibition of hyaluronidase activity. Hyaluronidase inhibition assay was performed as previously described (35). A reaction was performed by mixing 35 μl 1% dimethyl sulfoxide (DMSO), 5 μl DH-P or inhibitor control (1 mg/ml oleanolic acid) and 5 μl 1.5 U/ml hyaluronidase. Ethanol was used as a control. After the mixture had been incubated at 37˚C for 10 min, 5 μl 0.03% (w/v) hyaluronic acid in 300 mM sodium phosphate (pH 5.35) was added and further incubated at 37˚C for 45 min. Then, 5 μl acid albumin substrate [0.1% BSA (Sigma-Aldrich; cat. no. 12659) in 24 mM sodium acetate and 79 mM acetic acid (pH 3.75)] was added. The absorbance was determined at 600 nm and measured immediately following

the addition of the substrate and continuously for 10 min at room temperature. Each sample was run in triplicate. The hyaluronidase inhibition was calculated as follows: % Hyaluronidase inhibition=(1-$A_{sample}/A_{control}$) x100.

Cell culture and cytotoxicity. Human melanoma SK-MEL-28 cells (passage 14) were cultured at a seeding density of ~20,000 cells/cm^2 in 75 cm^2 flask in Eagle's Minimum Essential Medium (EMEM; ATCC; cat. no. 30-2003) supplemented with 10% fetal bovine serum (FBS) (Gibco; cat. no. 10270-106) and 1% penicillin/streptomycin. SK-MEL-28 cells (passage 15-22) were seeded in 96-well plates at a density of 5,000 cells/well and cultured for 24 h in EMEM. DH-P at final concentrations of 0, 10, 20, 30, 40, 50, 60, 80 or 100 μg/ml in 3.17% ethanol was added to each well. DMSO at a final concentration of 5% was used as an inhibitor control. Wells containing 3.17% ethanol at a final concentration served as controls. Cell cultures were maintained at 37˚C with 5% CO_2 throughout the treatment period. The experiments were performed twice independently with three replicates for each treatment. Following treatment for 96 h, 40 μl MTT solution was added and incubated at 37˚C for 3 h. After removing the supernatant, 50 μl 100% DMSO was added. The absorbance was measured at 570 nm. The cell viability was calculated as follows: % Cell viability=$A_{sample}/A_{control}$ x100. The half-maximal inhibitory concentration (IC_{50}) was determined from a dose response curve (GraphPad Software Version 10.3.1, Inc.; Dotmatics).

Wound healing assay. SK-MEL-28 cells were cultured in serum-free EMEM in 24-well plates at a density of $1x10^5$ cells/well (~80% confluency) at 37 ˚C for 24 h. After removing media, a gap in the middle of each well was created by scratching with a sterile 100-μl pipette tip. Loosely attached cells were removed using PBS (pH 7.4). Cells were treated with the DH-P at 20 μg/ml for 0, 24, 48, and 96 h. DMSO (5%) was used as an inhibitor control. A drug-free plate with 3.17% ethanol served as a control. Cell cultures were maintained at 37˚C with 5% CO_2 throughout the treatment period. The cell migration was photographed under a light microscope at 0, 24, 48 and 96 h after treatment. Gap distances were measured using ImageJ software Version 1.53v (National Institutes of Health). The experiment was performed twice independently with three replicates for each treatment.

Cell migration assay. Cell migration was assessed using the EZCell Cell Invasion Assay kit (Abcam; cat. no. ab287890) according to the manufacturer's instructions. Briefly, diluted human fibronectin solution at a 1:5 ratio was coated on the top chamber at 25˚C for 3 h. A total of ~$5x10^4$ cells in FBS-free EMEM were seeded in the top chamber with DH-P at 0.5 (10 μg/ml), 2/3 IC_{50} (13.3 μg/ml), and IC_{50} (20 μg/ml). Cells exposed to 3.17% ethanol served as controls. Then, 200 μl FBS-containing EMEM was added to the bottom chamber. The chamber was incubated at 37˚C in a humidified CO_2 incubator for 72 h according to the manufacturer's instructions. Cells that had migrated to the bottom chamber were stained with dissociation/dye solution at 37˚C with 5% CO_2 for 1 h. Each treatment was run in four replicates. The absorbance of the invaded cells was read at excitation/emission wavelengths of 535/587 nm using a fluorescence microplate reader (Tecan Group, Ltd.). The percentage of invasive cell numbers was calculated from a standard curve.

Analysis of nuclear morphology by Hoechst 33342 staining. SK-MEL-28 cells were seeded at a density of $3x10^5$ cells/well in a 35x10 mm dish chamber (SPL Life Sciences) for 24 h. Cells were treated with DH-P at 20 μg/ml for 0, 48 and 96 h. Dishes containing 3.17% ethanol and 5% DMSO were used as controls and inhibitor controls, respectively. Cells were incubated at 37˚C with 5% CO_2 during treatment. Cells were observed for DNA damage at 0, 48 and 96 h after treatment. After removing media, nuclei were stained with 10 μg/ml Hoechst 33342 (Sigma-Aldrich; Merck KGaA) in PBS (pH 7.4) at room temperature for 15 min in the dark, as previously described (36). The morphology of nuclei was examined using a fluorescence microscope at 40X magnification (Olympus Corporation). Each treatment was run in triplicate.

Gene expression analysis using reverse transcription-quantitative (RT-q)PCR. SK-MEL-28 cells were treated with DH-P at 20 μg/ml for 48 h. Cells exposed to 3.17% ethanol served as controls. Cells were incubated at 37˚C with 5% CO_2 during the treatment period. A total of ~$1x10^6$ cells/group was pooled and used to isolate total RNA with TRIzol reagent (Invitrogen; Thermo Fisher Scientific, Inc.). The cDNA was synthesized using a FIREScript RT cDNA Synthesis kit (Solis BioDyne). The cDNA samples were used as templates in the qPCR, while total RNA was used to screen for gDNA contamination. The qPCR reaction mixture was at a final volume of 20 μl containing 1X HOT FIREPol EvaGreen qPCR Mix Plus (NO-ROX; Solis BioDyne), 0.4 μM primer pair (Table I) and cDNA template (1 ng). Thermocycling conditions were as follows: Initial activation at 95˚C for 12 min, followed by 35 cycles of denaturation at 95˚C for 15 sec, annealing at primer-specific temperatures (Table I) for 20 sec and extension at 72˚C for 20 sec and final extension at 72˚C for 10 min. β-actin was used as the internal reference, and deionized water as the negative control. The experiments were performed independently twice, each with three biological replicates/treatment. Each gene from every sample was assessed in duplicate. The relative gene expression was determined using the comparative $2^{-\Delta\Delta Cq}$ method (37).

Statistical analysis. Data were analyzed using GraphPad Prism Version 10.3.1 (GraphPad Software, Inc.; Dotmatics). All data are presented as the mean ± SEM of ≥2 independent experimental repeats. One-way ANOVA followed by Dunnett's or Tukey's test was used to analyze inhibition of ECM activity and cell viability and migration, respectively. An unpaired t-test was performed in gene expression analysis. $P<0.05$ was considered to indicate a statistically significant difference.

Results

Detection and quantification of secondary metabolites in DH-P. Dendrobium accumulates large amounts of compounds beneficial to human health, especially polyphenols, flavonoids and alkaloids. Based on the TLC analysis, the two independent replications of DH-P had similar amounts and types

Table I. Primer pairs used to amplify genes involved in apoptosis via intrinsic pathway.

Gene	NCBI accession no.	Primer	Sequence, 5'→3'	Annealing temperature, ˚C	Amplicon size, bp
β-actin	HQ154074.1	Forward	CATCCTGCGTCTGGACCTGG	58	107
		Reverse	TAATGTCACGCACGATTTCC		
bax	JX524562.1	Forward	TCTGACGGCAACTTCAACTG	50.5	201
		Reverse	CGTCCCAAAGTAGGAGAGG		
bcl-2	KY098799.1	Forward	GAGGATTGTGGCCTTCTTTG	50.8	118
		Reverse	GTGCCGGTTCAGGTACTCAG		
caspase-3	NM_004346.4	Forward	TGGAATTGATGCGTGATGTT	48.2	161
		Reverse	ACTTCTACAACGATCCCCTC		
caspase-9	AF093130.1	Forward	GAGGGAGTCAGGCTCTTCCT	51.6	228
		Reverse	GCTCGACATCACCAAATCCT		
p53	AB082923.1	Forward	GTTCCGAGAGCTGAATGAGG	51.6	157
		Reverse	TGAGTCAGGCCCTTCTGTCT		

of compound (Fig. 1A). Violet and green fluorescence were observed in DH-P, indicating the presence of flavonoids and phenolics. However, quercetin (a common flavonol produced in plants) was not observed. Furthermore, total phenolics, flavonoids and alkaloids in DH-P were quantified and comprised 50.51±0.44, 80.11±0.69 and 38.75±1.77 μg/g fresh weight (FW), respectively (Fig. 1B).

Identification of tentative compounds in DH-P using UHPLC-ESI-QTOF-MS/MS. The present study used a targeted approach based on HR-MS (QTOF system) to investigate the chemical components in DH-P. The chromatographic separation and parameters were set according to separate detection methods for dendrobine (29), gigantol (30) and quercetin (31). These three targeted compounds were not detected in DH-P. In total, 119 compounds were matched using the MS2 spectra with the NIST Research Library v.2017. Each compound was then manually re-evaluated for mass error and searched for its functions. The focus was on compounds with biological activities such as anti-oxidant, anti-cancer, anti-inflammatory, anti-aging, depigmentation and anti-microbial activity. A total of eight tentative compounds of interest were identified using the detection method for quercetin (analyzed in a negative mode, with mass error <±5 ppm). The chemical formula, retention time, observed mass and calculated mass of the precursor ions, mass error and biological activity of compounds are summarized in Table II (38-45). The tentative compounds were guanosine, L-glutamine, threonic acid, quercetagetin, shikimic acid, D-(+)-mannose, *p*-coumaric acid and L-malic acid (Table II; Figs. 2 and S1).

Inhibition of free radicals. The effect of DH-P (25-10,000 μg/ml) on scavenging DPPH and ABTS radicals and reducing power for the ferric ion (Fe^{3+}) were investigated. Increased concentrations of DH-P had a greater inhibitory effect on DPPH and ABTS radicals, suggesting that the radical scavenging was concentration-dependent (Fig. 3A and B). However, DH-P scavenged ABTS radicals more effectively than DPPH. At the highest concentration (10,000 μg/ml), DH-P had VCEAC of 205.09±20.99 and 644.73±18.47 μg/ml for DPPH and ABTS radicals, respectively. A similar trend of scavenging performance was observed in the FRAP assay, suggesting that the inhibition was concentration-dependent (Fig. 3C). The highest concentration (10,000 μg/ml) of DH-P had a reducing power for Fe^{3+} equivalent to 465.83±31.37 FRAP value/μg extract. Consistent results across three different antioxidant assays validated the strong radical scavenging and reducing properties of DH-P.

Inhibition of collagenase and hyaluronidase activity. The present study investigated the effect of DH-P on the inhibition of enzymes responsible for degrading ECM components, such as collagenase and hyaluronidase (Fig. 4). DH-P inhibited the activity of collagenase and hyaluronidase, however, its inhibitory effects were less potent than those of the respective inhibitor controls, 1,10-PN and OA. DH-P significantly inhibited collagenase activity at 4,000-10,000 μg/ml, with a slight decrease in inhibitory effects as the concentration increased. DH-P at a concentration of 4,000 μg/ml exerted the maximum inhibitory activity for the collagenase enzyme (36.57±3.62%; Fig. 4A). The inhibitory activity of hyaluronidase was observed across DH-P concentrations 25-4,000 μg/ml with no significant difference, with the maximum inhibition being 41.52±3.49%; inhibition was significantly decreased by DH-P ≥6,000 μg/ml (Fig. 4B).

Inhibition of melanoma cell viability and migration. The cytotoxicity was evaluated on melanoma SK-MEL-28 cells treated with DH-P (0-100 μg/ml) for 96 h. The viability of SK-MEL-28 gradually decreased as the concentration of DH-P increased (Figs. 5A and S2). DH-P at 20 μg/ml significantly decreased viability of SK-MEL-28 cells. In addition, SK-MEL-28 cell viability was significantly inhibited when cells were exposed to DH-P ≥30 μg/ml (Fig. S2). DH-P had an IC_{50} value of 20.23±1.04 μg/ml (Fig. 5A). Therefore, DH-P at 20 μg/ml was applied for subsequent experiments.

Table II. Tentative compounds in DH-P identified using ultra-high-performance liquid chromatography-electrospray ionization-quadrupole time-of-flight tandem mass spectrometry and National Institute of Standards and Technology (NIST) research library v.2017.

Tentative Compound	Chemical formula	Retention time, min	Observed $[M-H]^-$, m/z	Calculated $[M-H]^-$, m/z	Mass error, ppm	Main MS2 fragments, m/z	Biological activity	(Refs.)
L-glutamine	$C_5H_{10}N_2O_3$	2.370	145.0622	145.0619	2.0681	127.0514; 84.0456	Anti-oxidant	(38)
D-(+)-mannose	$C_6H_{12}O_6$	2.462	179.0563	179.0561	1.1170	71.0139; 59.0140	Anti-cancer; anti-bacterial	(39)
Threonic acid	$C_4H_8O_5$	2.480	135.0302	135.0299	2.2217	75.0086; 59.0142	Stimulatory action on vitamin C uptake	(40)
Guanosine	$C_{10}H_{13}N_5O_5$	2.490	282.0847	282.0844	1.0635	150.0419; 133.0157; 108.0201	Anti-oxidant; anti-inflammatory	(41)
Shikimic acid	$C_7H_{10}O_5$	2.487	173.0450	173.0455	-2.8894	93.0343; 71.0140; 65.0398	Depigmentation	(42)
L-malic acid	$C_4H_6O_5$	2.527	133.0139	133.0142	-2.2554	115.0046; 72.9932; 71.0139	Anti-oxidant; anti-microbial	(43)
Quercetagetin	$C_{15}H_{10}O_8$	9.437	317.0306	317.0303	0.9463	151.0037; 109.0299	Anti-cancer	(44)
p-coumaric acid	$C_9H_8O_3$	9.560	163.0406	163.0401	3.0667	119.0507; 91.0179	Anti-oxidant; anti-microbial; anti-tumor; anti-inflammatory	(42, 45)

MS2, tandem mass spectrometry spectra; $[M-H]^-$, deprotonated molecule.

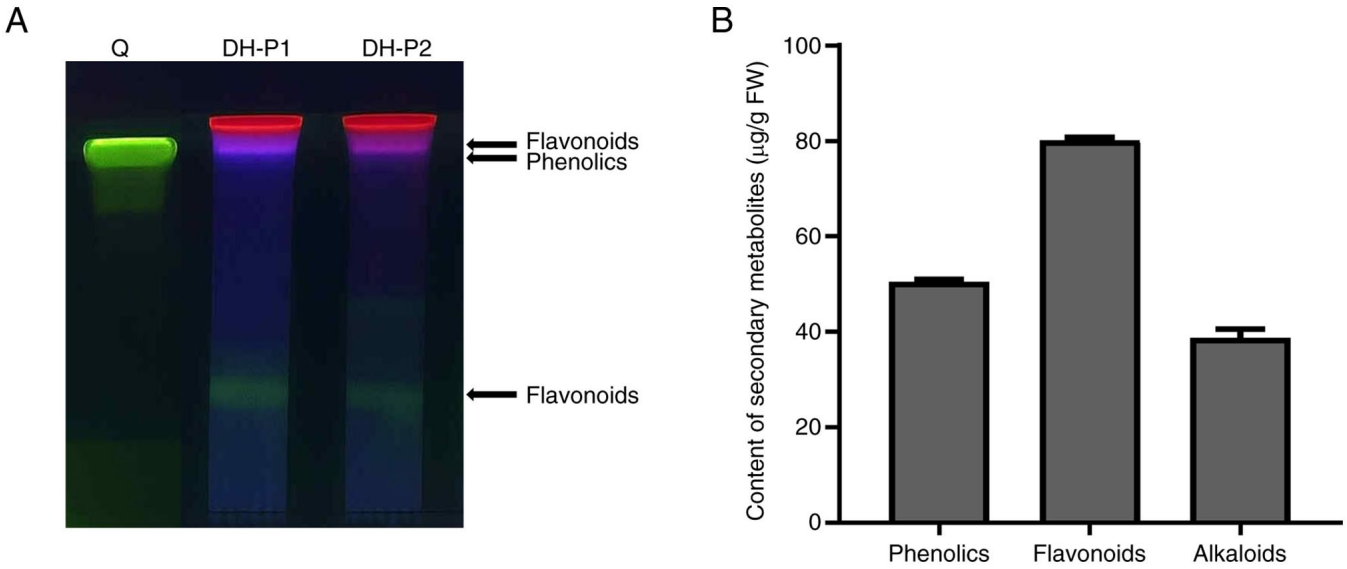

Figure 1. Determination of secondary metabolites in DH-P by thin layer chromatography. (A) Chromatogram of phenolic and flavonoid compounds in DH-P (10 mg/ml). (B) Amounts of total phenolics, flavonoids and alkaloids in DH-P. n=6. DH-P, propanolic extract from *Dendrobium* Pearl Vera hybrid; Q, quercetin; FW, fresh weight.

Cells treated with 20 μg/ml DH-P migrated at a similar rate as the control group at all time points, while 5% DMSO (inhibitor control) inhibited cell migration (Figs. 5B and S3). In addition, there was no significant difference in the invaded cell number between DH-P at all concentrations and the control group, suggesting that DH-P had no inhibitory effect on migration of SK-MEL-28 cells (Fig. 5C).

Analysis of cell apoptosis. As DH-P could inhibit viability of SK-MEL-28 cells, cell death induced through apoptosis was investigated. Hoechst staining was performed to observe cell and nuclear morphological changes (Fig. 6). Following exposure to DH-P at 20 μg/ml for 48 and 96 h, nuclei were condensed or fragmented. In addition, the cell number decreased notably compared with the control group. Furthermore, cells treated with 5% DMSO (inhibitor

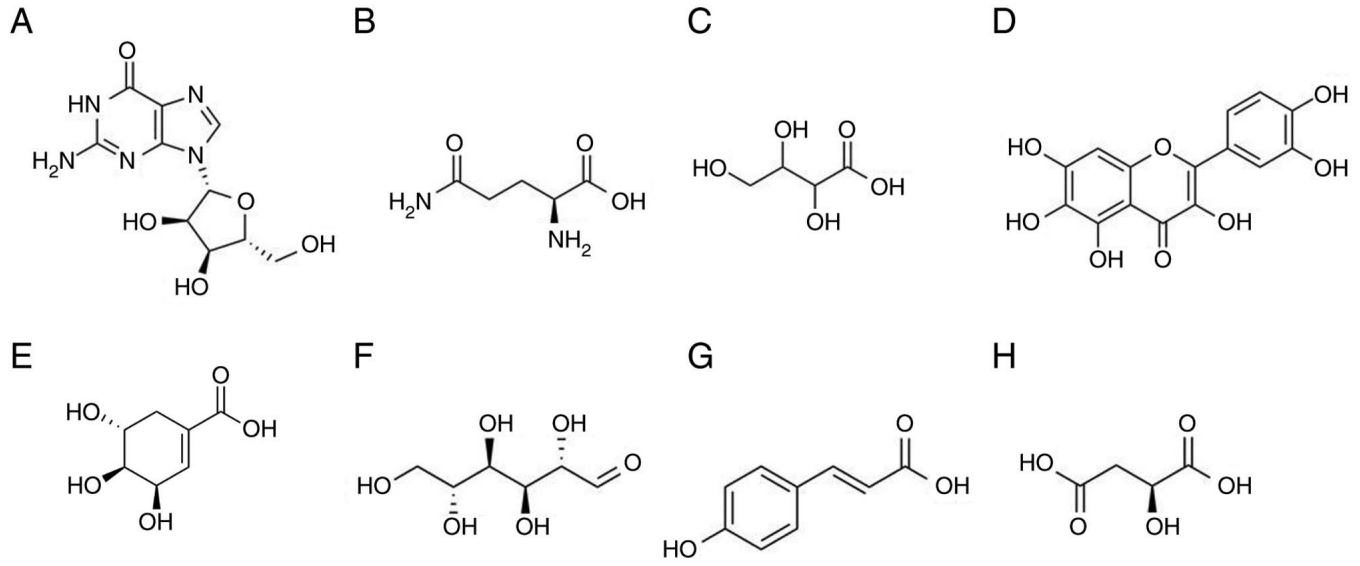

Figure 2. Structures of tentative compounds identified in propanolic extract from *Dendrobium* Pearl Vera hybrid. (A) Guanosine. (B) L-glutamine. (C) Threonic acid. (D) Quercetagetin. (E) Shikimic acid. (F) D-(+)-mannose. (G) *p*-coumaric acid. (H) L-malic acid.

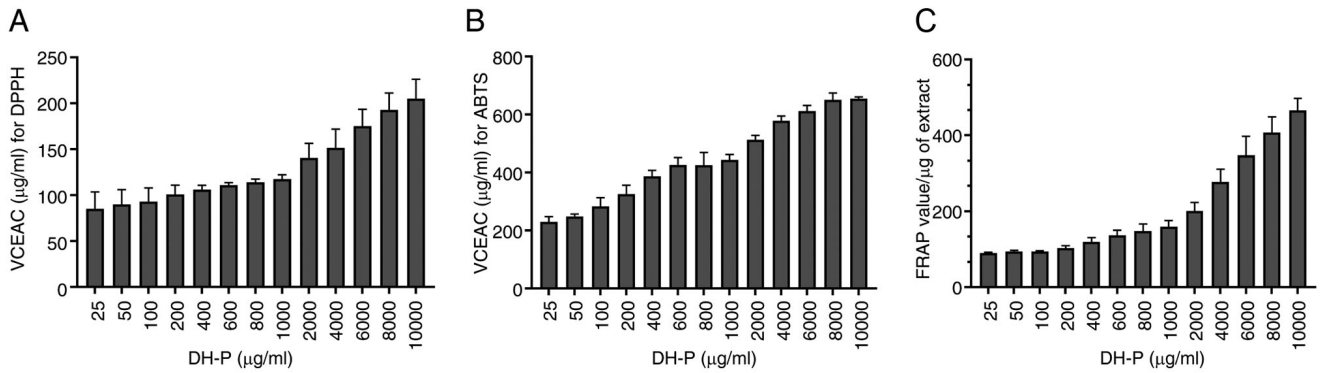

Figure 3. Scavenging effect of DH-P on free radicals at various concentrations. Radical scavenging capacity of DH-P for (A) DPPH and (B) ABTS radicals. (C) Reducing power on ferric ions (Fe^{3+}). n=6. DH-P, propanolic extract from *Dendrobium* Pearl Vera hybrid; DPPH, 2,2-diphenyl-1-picrylhydrazyl; ABTS, 2,2'-Azino-bis(3-ethylbenzothiazoline-6-sulfonic acid); VCEAC, vitamin C equivalent antioxidant capacity.

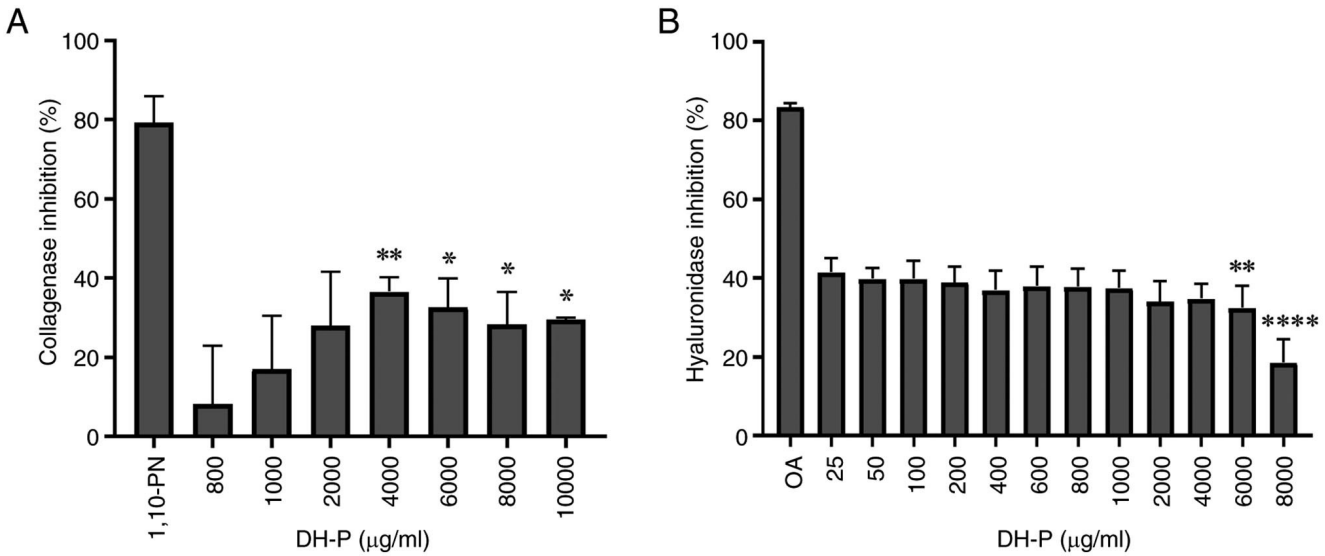

Figure 4. Effect of DH-P on extracellular matrix enzyme activity at various concentrations. Inhibitory effects of DH-P on (A) collagenase and (B) hyaluronidase enzyme activity. Inhibitor controls were 1 M 1,10-PN and 1 mg/ml OA. n=6. *P<0.05; **P<0.01; ****P<0.0001 vs. 800 or 25 μg/ml DH-P. OA, oleanolic acid; DH-P, propanolic extract from *Dendrobium* Pearl Vera hybrid; 1,10-PN, 1,10-phenanthroline.

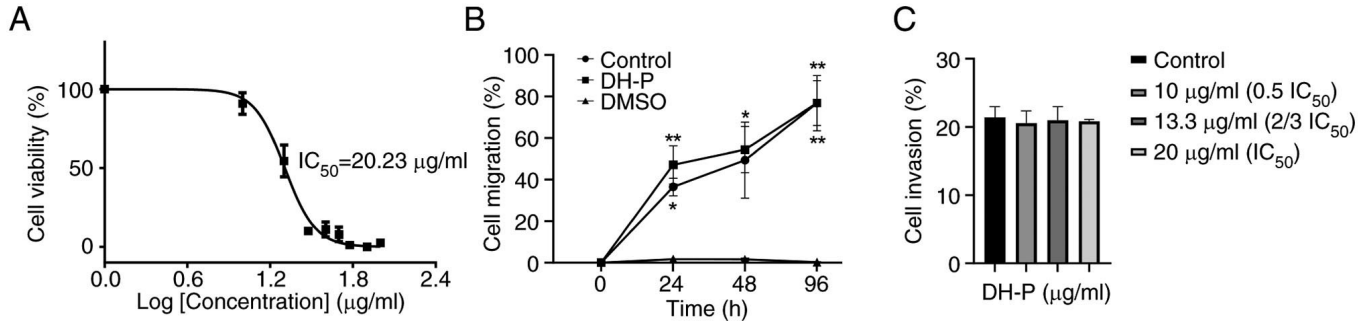

Figure 5. Inhibitory effects of DH-P on cell viability and migration. (A) IC_{50} value determined from dose-response cytotoxicity analysis of DH-P (0-100 μg/ml). (B) Quantitative analysis of SK-MEL-28 cell migration following treatment with 20 μg/ml DH-P or 5% DMSO. n=6. *P<0.05; **P<0.01; vs. DMSO. (C) Transwell migration assay of SK-MEL-28 cells treated with DH-P for 72 h (n=4). DH-P, propanolic extract from *Dendrobium* Pearl Vera hybrid; IC_{50}, half-maximal inhibitory concentration.

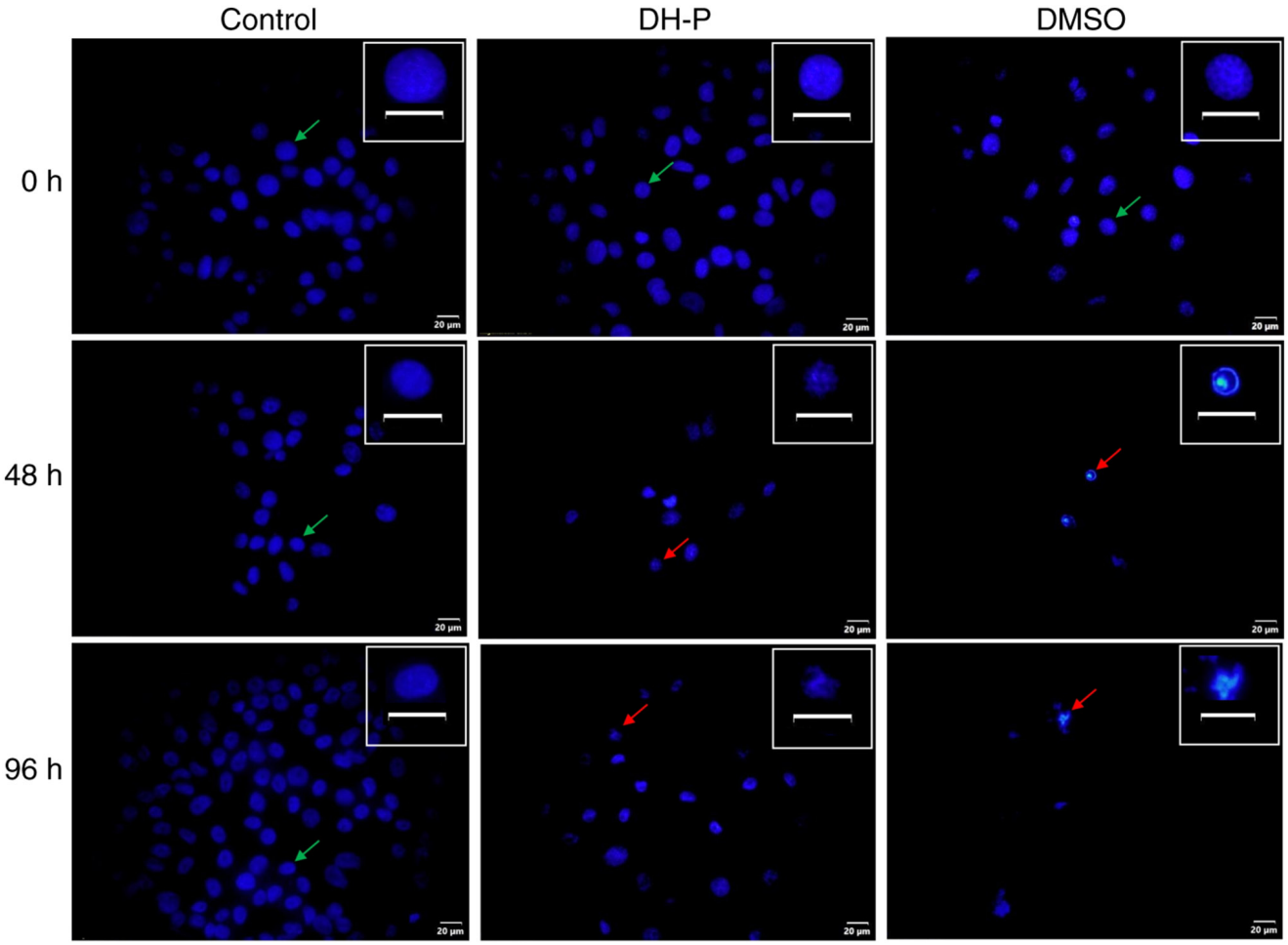

Figure 6. Nuclear morphology of SK-MEL-28 cells treated with DH-P at 20 μg/ml for 0, 48, and 96 h. Nuclei were stained using Hoechst 33342 (magnification, x40). Scale bar, 20 μm. Green arrow, nuclei of healthy cells. Red arrow, condensed or fragmented nuclei of apoptotic cells. DH-P, propanolic extract from *Dendrobium* Pearl Vera hybrid.

control) were decreased in number, and the nuclei were fragmented.

The expression of genes involved in intrinsic apoptosis was evaluated to confirm whether cell death was induced through apoptosis (Fig. 7). The relative fold-changes in the expression of the apoptotic genes *bax*, *bcl-2*, *cytc*, *cas-3*, *cas-9* and *p53* were 1.035, 0.858, 1.558, 2.650, 2.813 and 1.195, respectively, compared with the control group. Only *cas-3* and *cas-9* were significantly upregulated by DH-P. There was no significant change in the expression of *bax*, *bcl-2*, *cytc* and *p53*.

Discussion

Dendrobium spp. is a large genus with >1,000 species (3). *Dendrobium* contains high amounts of bioactive compounds, such as polyphenols, flavonoids, alkaloids and polysaccharides,

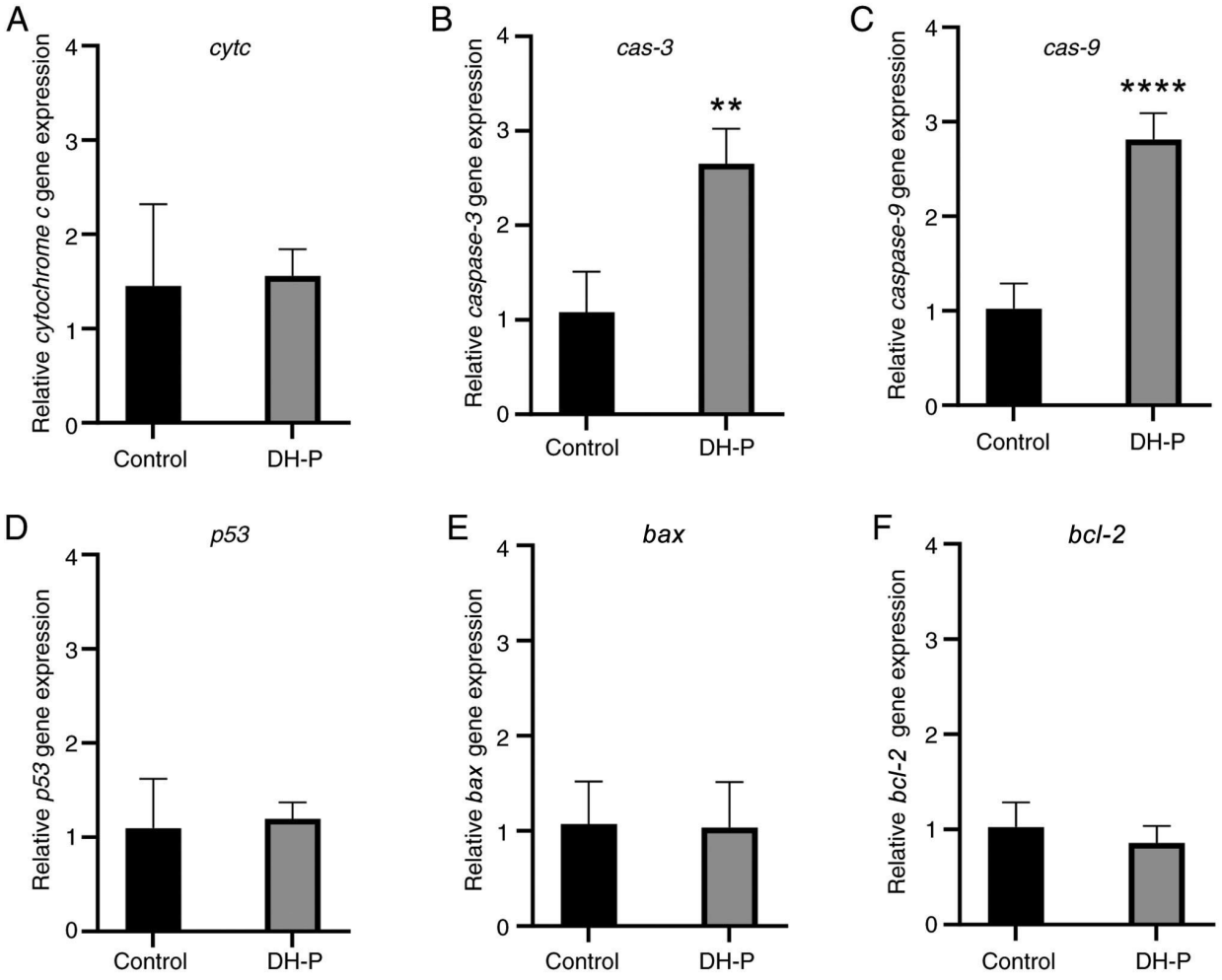

Figure 7. Expression of apoptotic-related genes in SK-MEL-28. Fold-change in cells treated with DH-P at 20 μg/ml for 48 h were calculated relative to control group. (A) *cytc*. (B) *cas-3*. (C) *cas-9*. (D) *p53*. (E) *bax*. (F) *bcl-2*. n=6. **P<0.01; ****P<0.0001 vs. control. DH-P, propanolic extract from *Dendrobium* Pearl Vera hybrid; *cytc*, cytochrome c; *cas*, caspase.

which confer biological activities beneficial for human health and wellness (4,17,46). *Dendrobium* Pearl Vera is a hybrid whose genetic material is derived from *D. bigibbum* (93.75%) and *D. canaliculatum* (6.25%), which are used as cosmetic ingredients and a treatment for sores, respectively (24,46). The present findings agreed with several reports on *Dendrobium* benefits (3-8,30), especially for skin treatment and health improvement, revealing that *Dendrobium* Pearl Vera accumulates phenolics, flavonoids and alkaloids. These bioactive compounds exert key biological effects, such as anti-oxidant, anti-aging, and anti-cancer properties (2,4-6). Crude extracts from DH plant at 1 mg/ml exhibited scavenging activity and human tyrosinase inhibition (24). In addition, DH-P at various concentrations demonstrated inhibition of free radicals and enzyme activity involved in ECMs degradation, as well as induction of melanoma cell apoptosis, which may be attributed to its bioactive compounds.

Reactive oxygen species (ROS) serve a key role in cancer growth and development. Elevated ROS levels promote proliferation and metastasis, thereby contributing to cancer progression (5,47). DH-P contains secondary metabolites that may serve as free radical scavengers or metal ion chelators (24), suggesting its bioactive components may inhibit SK-MEL28 cell proliferation by reducing ROS levels. In addition, dysregulation of metal homeostasis, such as iron, may mediate the production of ROS and alter MMP activity, causing destruction of the cell membrane leading to skin aging and malignant cancer (47-49). DH-P also affected the activity of collagenase and hyaluronidase. Skin aging and cancer progression occur via decreased skin strength and resiliency, mostly due to alteration of the ECM biomolecules such as collagen, elastin and HA (11,13,49). Among these, collagen fibrils, the most abundant structural protein in the skin, are particularly degraded by collagenases and other MMPs (12,49). Hydrophilic ECM biomolecules, including the non-sulfated glycosaminoglycan and HA, may be present in lower quantities under physiological conditions, but the increase of HA significantly affects the progression and metastasis of cancer cells (13). Phenolic and flavonoids protect against skin destruction and hyperpigmentation by inhibiting the enzymes involved in the degradation of EMC biomolecules as well as inhibiting the melanin production by melanoma cells (24,50). *Dendrobium* Pearl Vera accumulates bioactive secondary metabolites; therefore, the extract may also protect skin damage from pollutants and sunlight exposure, which are common stimuli for the generation of free radicals and an

increase in dermal EMC-degrading enzyme activity. DH-P at 4,000 μg/ml exerted maximal collagenase activity inhibition and maintained hyaluronidase activity, suggesting this dose may prolong the structural integrity of ECM. It has been reported that *D. crepidatum* contains bibenzyl derivatives, polyphenols and flavonoids that exert antioxidant and cytotoxic effects on HeLa (human cervical carcinoma) and U251 (human glioblastoma) cancer cell lines (6). Alkaloids have medicinal properties, especially for cancer prevention, and are commonly found in orchids, including *Dendrobium* Pearl Vera, with most alkaloids in orchids being classified either as pyrrolizidines or dendrobines (51).

To the best of our knowledge, few bioactive compounds have been reported with antioxidant and anticancer activity in DH-P, such as 3,5-di-tert-butyl-4-hydroxybenzaldehyde, 5-hydroxymethyl-2-furaldehyde, 4-guanidinobutyric acid, L-norleucine and acetophenone (24). Notably, the present study expanded the chemical components in DH-P to identify other chemicals, using QTOF. A total of eight tentative compounds [guanosine, L-glutamine, threonic acid, quercetagetin, shikimic acid, D-(+)-mannose, *p*-coumaric acid, and L-malic acid] were identified with beneficial activities for skin and medicinal use, such as anti-oxidant, anti-aging, anti-microbial anti-cancer, anti-inflammatory and whitening effects. The therapeutic potential of plant-derived derivatives may be attributed to combined action of diverse active phytochemicals with varying chemical structures that act synergistically to enhance biological activities (44,52). Based on the present TLC analysis, flavonoids and phenolics were detected in varying amounts and types. Notably, different plant species may exhibit variations in fluorescent spot coloration (25,53). The strong inhibitory effect of DH-P on SK-MEL-28 cell viability may result from the interactions among its constituent compounds.

Several reports suggested that extracts from *Dendrobium* spp. inhibit proliferation and metastasis on various types of cancer cell (4,6,17); to the best of our knowledge, however, research is limited on the inhibitory effects of *Dendrobium* extract on skin cancer cells (10,24,36). Cytotoxic effects against cancer cells are classified as 'very active', 'active', 'moderately active' or 'no cytotoxic activity' when the IC_{50} value is <10, 10-100, 101-500 or >500 μg/ml, respectively (54). Based on the IC_{50} value (20.23 μg/ml) of DH-P for SK-MEL-28 cells, it was classified as an active inhibitor toward human melanoma cells. By contrast, SK-MEL-28 cells that survived treatment with 20 μg/ml DH-P could migrate and invade at the same rate as the control group at all time points, implying the progression and aggressiveness of escaping melanoma cells. SK-MEL-28 is a malignant melanoma cell line and represents the most aggressive form of skin cancer (9,10). Malignant cell migration and invasion are the primary manifestations of tumor biology and key components of metastasis, which is a notable cause of death in oncology patients (55).

Apoptosis is a form of programmed cell death occurring naturally and is induced in cancer cells by natural compounds (17-22). Bioactive compounds, such as quercetin, prevent the cell cycle progression, inhibit cell proliferation and promote cell apoptosis in numerous types of cancer, such as lung, colorectal, pancreatic, breast and prostate cancer (56). The extracts from *D. draconis*, *D. falconeri*, *D. findlayanum*, *D. loddigesii*, as well as *Dendrobium* Pearl Vera, exhibit anti-cancer activity (14). Cell apoptosis is characterized by cell shrinkage and chromatin condensation and fragmentation that produces compact nuclei and/or the formation of apoptotic bodies (44). Decreased cell number and fragmentation of nuclei were observed in SK-MEL-28 cells treated with DH-P, suggesting cell apoptosis might have occurred (36). In addition, the mRNA expression of apoptotic executors *cas-9* and *cas-3* significantly increased in SK-MEL-28 cells treated with DH-P, demonstrating that cell death was caused by apoptosis. The caspases are a family of cysteine proteases and key mediators of apoptosis. Cas-8 and -9 are determinants in the extrinsic and intrinsic pathway, respectively. Cas-3 is key for apoptotic chromatin condensation and DNA fragmentation (44). Although the expression levels of *bax*, *bcl-2*, *cytc* and *p53* were unchanged, the significant increase of *cas-9* and *cas-3* expression demonstrated a hallmark of apoptosis via the intrinsic pathway. Polysaccharides from *D. officinale* induce apoptosis in Saos-2 osteosarcoma cells via the intrinsic pathway, with no change in p53, Bax and Cas-9 protein levels, but an increase in Cas-3 expression (21). Certain compounds in *Dendrobium*, such as moscatilin and quercetin, exert anti-cancer effects on melanoma cells and induce cell apoptosis via the intrinsic pathway (17,23). Quercetagetin was identified in DH-P and has been reported to induce the apoptotic process through the intrinsic apoptotic pathway in cervical (CaSki), breast (MDA-MB-231) and lung (SK-Lu-1) cancer cells (44).

In conclusion, based on the inhibitory effects of DH-P on free radicals, ECM enzymes and SK-MEL-28 cell proliferation, *Dendrobium* Pearl Vera is a promising natural candidate as an anti-oxidant and for skin cancer prevention as an anti-cancer agent.

Acknowledgements

The authors would like to thank CordyBiotech Co., Ltd. for providing plant material.

Funding

The present study was supported by Basic Research Fund (grant no. BRF5/2567) and International SciKU Branding (ISB), Faculty of Science, Kasetsart University, Bangkok, Thailand.

Availability of data and materials

The data generated in the present study may be found in Figshare under accession number 10.6084/m9.figshare.30204490 at the following URL: doi.org/10.6084/m9.figshare.30204490).

Authors' contributions

RK and PM performed the experiments. RK, PM, and AA designed the experiments, analyzed and interpreted the data, and wrote the manuscript. PK, NPT, NMS, WP and PW conceived the study and analyzed data. AA and PW confirm the authenticity of all the raw data. All authors have read and approved the final manuscript.

Ethics approval and consent to participate

Not applicable.

Patient consent for publication

Not applicable.

Competing interests

The authors declare they have no competing interests.

References

1. Givnish TJ, Spalink D, Ames M, Lyon SP, Hunter SJ, Zuluaga A, Iles WJD, Clements MA, Arroyo MTK, Leebens-Mack J, *et al*: Orchid phylogenomics and multiple drivers of their extraordinary diversification. Proc R Soc B 282: 20151553, 2015.
2. Minh TN, Khang do T, Tuyen PT, Minh LT, Anh LH, Quan NV, Ha PT, Quan NT, Toan NP, Elzaawely AA and Xuan TD: Phenolic compounds and antioxidant activity of phalaenopsis orchid hybrids. Antioxidants (Basel) 5: 31, 2016.
3. Moretti M, Cossignani L, Messina F, Dominici L, Villarini M, Curini M and Marcotullio MC: Antigenotoxic effect, composition and antioxidant activity of *Dendrobium speciosum*. Food Chem 140: 660-665, 2013.
4. Cakova V, Bonte F and Lobstein A: *Dendrobium*: Sources of active ingredients to treat age-related pathologies. Aging Dis 8: 827-849, 2017.
5. Tungmunnithum D, Thongboonyou A, Pholboon A and Yangsabai A: Flavonoids and other phenolic compounds from medicinal plants for pharmaceutical and medical aspects: An overview. Medicines (Basel) 5: 93, 2018.
6. Paudel MR, Chand MB, Pant B and Pant B: Assessment of antioxidant and cytotoxic activities of extracts of *Dendrobium crepidatum*. Biomolecules 9: 478, 2019.
7. Luo A, He X, Zhou S, Fan Y, He T and Chun Z: In vitro antioxidant activities of a water-soluble polysaccharide derived from *Dendrobium nobile* Lindl. extracts. Int J Biol Macromol 45: 359-363, 2009.
8. Luo A, Ge Z, Fan Y, Luo A, Chun Z and He X: In vitro and in vivo antioxidant activity of a water-soluble polysaccharide from *Dendrobium denneanum*. Molecules 16: 1579-1592, 2011.
9. Roky AH, Islam MM, Ahasan AMF, Mostaq MS, Mahmud MZ, Amin MN and Mahmud MA: Overview of skin cancer types and prevalence rates across continents. Cancer Pathog Ther 3: 89-100, 2024.
10. Daveri E, Valacchi G, Romagnoli R, Maellaro E and Maioli E: Antiproliferative effect of rottlerin on Sk-Mel-28 melanoma cells. Evid Based Complement Alternat Med 2015: 545838, 2015.
11. Moro N, Mauch C and Zigrino P: Metalloproteinases in melanoma. Eur J Cell Biol 93: 23-29, 2014.
12. Kessenbrock K, Plaks V and Werb Z: Matrix metalloproteinases: Regulators of the tumor microenvironment. Cell 141: 52-67, 2010.
13. Karousou E, Parnigoni A, Moretto P, Passi A, Viola M and Vigetti D: Hyaluronan in the cancer cells microenvironment. Cancers (Basel) 15: 798, 2023.
14. Ghai D, Verma J, Kaur A, Thakur K, Pawar S and Sembi J: Bioprospection of orchids and appraisal of their therapeutic indications. In: Bioprospecting of plant biodiversity for industrial molecules. Santosh KU and Sudhir PS (eds.) John Wiley & Sons, West Sussex, pp464, 2021.
15. Zhao X, Sun P, Qian Y and Suo H: *D. candidum* has in vitro anticancer effect in HCT-116 cancer cells and exerts in vivo anti-metastratic effects in mice. Nutr Res Pract 8: 487-493, 2014.
16. Prasad R and Koch B: Antitumor activity of ethanolic extract of *Dendrobium formosum* in T-cell lymphoma: An in vitro and in vivo study. Biomed Res Int 2014: 753451, 2014.
17. Cardile V, Avola R, Graziano ACE and Russo A: Moscatilin, a bibenzyl derivative from the orchid *Dendrobium loddigesii*, induces apoptosis in melanoma cells. Chem Biol Interact 323: 109075, 2020.
18. Robertson JD and Orrenius S: Molecular mechanisms of apoptosis induced by cytotoxic chemicals. Crit Rev Toxicol 30: 609-627, 2000.
19. Li Y, Zhang S, Geng JX and Hu XY: Curcumin inhibits human non-small cell lung cancer A549 cell proliferation through regulation of Bcl-2/Bax and cytochrome C. Asian Pac J Cancer Prev 14: 4599-4602, 2013.
20. Zhao Y, Liu Y, Lan XM, Xu GL, Sun YZ, Li F and Liu HN: Effect of *Dendrobium officinale* extraction on gastric carcinogenesis in rats. Evid Based Complement Alternat Med 2016: 1213090, 2016.
21. Zhang X, Duan S, Tao S, Huang J, Liu C, Xing S, Ren Z, Lei Z, Li Y and Wei G: Polysaccharides from *Dendrobium officinale* inhibit proliferation of osteosarcoma cells and enhance cisplatin-induced apoptosis. J Funct Foods 73: 104143, 2020.
22. Zhang Y, Zhang Q, Xin W, Liu N and Zhang H: Nudol, a phenanthrene derivative from *Dendrobium nobile*, induces cell cycle arrest and apoptosis and inhibits migration in osteosarcoma cells. Drug Des Devel Ther 13: 2591-2601, 2019.
23. Reyes-Farias M and Carrasco-Pozo C: The anti-cancer effect of quercetin: Molecular implications in cancer metabolism. Int J Mol Sci 20: 3177, 2019.
24. Swainson NM, Pengoan T, Khonsap R, Meksangsee P, Hagn G, Gerner C and Aramrak A: In vitro inhibitory effects on free radicals, pigmentation, and skin cancer cell proliferation from *Dendrobium* hybrid extract: A new plant source of active compounds. Heliyon 9: e20197, 2023.
25. Maliński MP, Kikowska MA, Soluch A, Kowalczyk M, Stochmal A and Thiem B: Phytochemical screening, phenolic compounds and antioxidant activity of biomass from *Lychnis flos-cuculi* L. in vitro cultures and intact plants. Plants (Basel) 10: 206, 2021.
26. Attard E: A rapid microtitre plate Folin-Ciocalteu method for the assessment of polyphenols. Cent Eur J Biol 8: 48-53, 2013.
27. Bhattacharyya P, Kumaria S, Diengdoh R and Tandon P: Genetic stability and phytochemical analysis of the in vitro regenerated plants of *Dendrobium nobile* Lindl., an endangered medicinal orchid. Meta Gene 2: 489-504, 2014.
28. Shamsa F, Monsef H, Ghamooshi R and Verdian-rizi M: Spectrophotometric determination of total alkaloids in some Iranian medicinal plants. Thai J Pharm Sci 32: 17-20, 2008.
29. Sarsaiya S, Jain A, Fan X, Jia Q, Xu Q, Shu F, Zhou Q, Shi J and Chen J: New insights into detection of a dendrobine compound from a novel endophytic *Trichoderma longibrachiatum* strain and its toxicity against phytopathogenic bacteria. Front Microbiol 11: 337, 2020.
30. Chan CF, Wu CT, Huang WY, Lin WS, Wu HW, Huang TK, Chang MY and Lin YS: Antioxidation and melanogenesis inhibition of various *Dendrobium tosaense* extracts. Molecules 23: 1810, 2018.
31. Kızıltaş H, Bingöl Z, Gören A, Alwasel SH and Gülçin I: Anticholinergic, antidiabetic and antioxidant activities of *Ferula orientalis* L. determination of its polyphenol contents by LC-HRMS. Rec Nat Prod 15: 513-528, 2021.
32. Herald TJ, Gadgil P and Tilley M: High-throughput micro plate assays for screening flavonoid content and DPPH-scavenging activity in sorghum bran and flour. J Sci Food Agric 92: 2326-2331, 2012.
33. Thaipong K, Boonprakob U, Crosby K, Cisneros-Zevallos L and Byrne DH: Comparison of ABTS, DPPH, FRAP, and ORAC assays for estimating antioxidant activity from guava fruit extracts. J Food Compos Anal 19: 669-675, 2006.
34. Bolanos de la Torre AA, Henderson T, Nigam PS and Owusu-Apenten RK: A universally calibrated microplate ferric reducing antioxidant power (FRAP) assay for foods and applications to Manuka honey. Food Chem 174: 119-123, 2015.
35. Nema NK, Maity N, Sarkar BK and Mukherjee PK: Matrix metalloproteinase, hyaluronidase and elastase inhibitory potential of standardized extract of *Centella asiatica*. Pharm Biol 51: 1182-1187, 2013.
36. Wu Y, Zhang P, Yang H, Ge Y and Xin Y: Effects of demethoxycurcumin on the viability and apoptosis of skin cancer cells. Mol Med Rep 16: 539-546, 2017.
37. Livak KJ and Schmittgen TD: Analysis of relative gene expression data using real-time quantitative PCR and the 2(-Delta Delta C(T)) method. Methods 25: 402-408, 2001.
38. Takaoka M, Okumura S, Seki T and Ohtani M: Effect of amino-acid intake on physical conditions and skin state: A randomized, double-blind, placebo-controlled, crossover trial. J Clin Biochem Nutr 65: 52-58, 2019.
39. Chen S, Wang K and Wang Q: Mannose: A promising player in clinical and biomedical applications. Curr Drug Deliv 15: 1435-1444, 2024.

40. Wang HY, Hu P and Jiang J: Pharmacokinetics and safety of calcium L-threonate in healthy volunteers after single and multiple oral administrations. Acta Pharmacol Sin 32: 1555-1560, 2011.
41. Bettio LE, Gil-Mohapel J and Rodrigues AL: Guanosine and its role in neuropathologies. Purinergic Signal 12: 411-426, 2016.
42. Chen YH, Huang L, Wen ZH, Zhang C, Liang CH, Lai ST, Luo LZ, Wang YY and Wang GH: Skin whitening capability of shikimic acid pathway compound. Eur Rev Med Pharmacol Sci 20: 1214-1220, 2016.
43. Borah HJ, Borah A, Yadav A and Hazarika S: Extraction of malic acid from *Dillenia indica* in organic solvents and its antimicrobial activity. Sep Sci Technol 58: 314-325, 2023.
44. Alvarado-Sansininea JJ, Sánchez-Sánchez L, López-Muñoz H, Escobar ML, Flores-Guzmán F, Tavera-Hernández R and Jiménez-Estrada M: Quercetagetin and patuletin: Antiproliferative, necrotic and apoptotic activity in tumor cell lines. Molecules 23: 2579, 2018.
45. Pei K, Ou J, Huang J and Ou S: *p*-Coumaric acid and its conjugates: Dietary sources, pharmacokinetic properties and biological activities. J Sci Food Agric 96: 2952-2962, 2016.
46. Wang YH: Traditional uses and pharmacologically active constituents of *Dendrobium* plants for dermatological disorders: A review. Nat Prod Bioprospect 11: 465-487, 2021.
47. Shen T, Wang Y, Cheng L, Bode AM, Gao Y, Zhang S, Chen X and Luo X: Oxidative complexity: The role of ROS in the tumor environment and therapeutic implications. Bioorg Med Chem 127: 118241, 2025.
48. Ying JF, Lu ZB, Fu LQ, Tong Y, Wang Z, Li WF and Mou XZ: The role of iron homeostasis and iron-mediated ROS in cancer. Am J Cancer Res 11: 1895-1912, 2021.
49. Cole MA, Quan T, Voorhees JJ and Fisher GJ: Extracellular matrix regulation of fibroblast function: Redefining our perspective on skin aging. J Cell Commun Signal 12: 35-43, 2018.
50. Kanlayavattanakul M, Lourith N and Chaikul P: Biological activity and phytochemical profiles of *Dendrobium*: A new source for specialty cosmetic materials. Ind Crops Prod 120: 61-70, 2018.
51. Śliwiński T, Kowalczyk T, Sitarek P and Kolanowska M: Orchidaceae-derived anticancer agents: A review. Cancers (Basel) 14: 754, 2022.
52. Pezzani R, Salehi B, Vitalini S, Iriti M, Zuñiga FA, Sharifi-Rad J, Martorell M and Martins N: Synergistic effects of plant derivatives and conventional chemotherapeutic agents: An update on the cancer perspective. Medicina (Kaunas) 55: 110, 2019.
53. Bernardi T, Bortolini O, Massi A, Sacchetti G, Tacchini M and De Risi C: Exploring the synergy between HPTLC and HPLC-DAD for the investigation of wine-making by-products. Molecules 24: 3416, 2019.
54. Yuliet S, Nurfajar R, Sindia S, Khaerati K and Saraswaty V: Immunomodulatory activity of Pepolo (*Bischofia javanica* Blume) stem bark ethanolic extract in *Staphylococcus aureus*-stimulated macrophages and anticancer activity against MCF-7 cancer cells. J Appl Pharm Sci 12: 109-116, 2022.
55. Wu JS, Jiang J, Chen BJ, Wang K, Tang YL and Liang XH: Plasticity of cancer cell invasion: Patterns and mechanisms. Transl Oncol 14: 100899, 2021.
56. Tang SM, Deng XT, Zhou J, Li QP, Ge XX and Miao L: Pharmacological basis and new insights of quercetin action in respect to its anti-cancer effects. Biomed Pharmacother 121: 109604, 2020.